

Trap-Seeking or Trap-Digging? Photojunction of Hydrated Electrons into Aqueous NaCl Solutions

Wilberth A. Narvaez, Eric C. Wu, Sanghyun J. Park, Mariah Gomez, and Benjamin J. Schwartz*



Cite This: *J. Phys. Chem. Lett.* 2022, 13, 8653–8659



Read Online

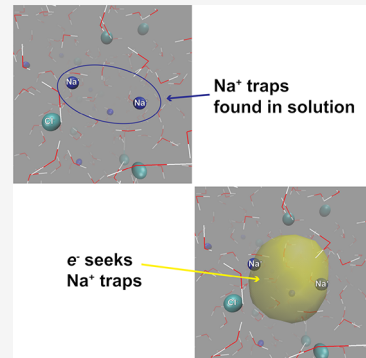
ACCESS |

Metrics & More

Article Recommendations

Supporting Information

ABSTRACT: It is well-known that when excess electrons are injected into an aqueous solution, they localize and solvate in ~ 1 ps. Still debated is whether localization occurs via “trap-digging”, in which the electron carves out a suitable localization site, or by “trap-seeking”, where the electron prefers to localize at pre-existing low-energy trap sites in solution. To distinguish between these two possible mechanisms, we study the localization dynamics of excess electrons in aqueous NaCl solutions using both ultrafast spectroscopy and mixed quantum-classical molecular dynamics simulations. By introducing pre-existing traps in the form of Na^+ ions, we can use the cation-induced blue-shift of the hydrated electron’s absorption spectrum to directly monitor the site of electron localization. Our experimental and computational results show that the electron prefers to localize directly at the sites of Na^+ traps; the presence of concentrated electrolytes otherwise has little impact on the way trap-seeking hydrated electrons relax following injection.



Since hydrated electrons (e_{aq}^- ’s) were first observed nearly six decades ago,¹ they have become a paradigm system for comparing the results of mixed quantum/classical (MQC)^{2–6} or ab initio^{7–11} simulations with ultrafast spectroscopic experiments.^{12–15} Of particular interest is the way in which hydrated electrons localize and equilibrate after they are injected into liquid water either via pulse radiolysis or multiphoton ionization. Ultrafast spectroscopy experiments show that following injection, excess electrons in liquid water first form an infrared-absorbing species on a 110–280 fs time scale, sometimes referred to as the “wet” electron, which subsequently converts into an equilibrated e_{aq}^- after 240–540 fs.^{12,13,15,16} Several groups have performed simulations to determine why hydrated electron equilibration takes place on sub-picosecond time scales.^{7,8,17–19} Some simulations investigating the rapidity of the e_{aq}^- ’s solvation have argued that the electrons are trapped by local potential fluctuations in the solvent or are “trap-seeking”. The idea is that liquid water contains pre-existing structures that are energetically predisposed to accommodate excess electrons and that the electrons prefer to localize in these places, where there is a lower barrier to equilibration.^{20–23} There is also the possibility that excess electrons in liquid water can localize and equilibrate in any kinetically accessible convenient spot, so that electrons are “trap-digging”.

The evidence for trap-seeking or trap-digging behavior of solvated electrons is varied. In liquid tetrahydrofuran (THF), the kinetics of injected electron equilibration in the presence of traps (either sodium cations or small amounts of added water) are relatively slow, with clear evidence for electron solvation in regions free of traps at early times, showing that such solvated

electrons are trap digging.^{24,25} On the other hand, Mostafavi and co-workers showed that, in mixtures of *n*-tributyl phosphate (TBP) and water, electrons prefer to solvate in water rather than TBP, which hints at trap-seeking behavior,²⁶ although the time resolution of the pulse radiolysis they used does not provide direct information on the primary localization step. Thus, there has been no way to experimentally determine which description, if either, is the most appropriate for electrons injected in liquid water that is not part of a mixture.

The key to distinguishing the mechanism by which hydrated electrons localize is to introduce pre-existing traps that are spectroscopically distinct from nontrapped e_{aq}^- ’s. Here, we provide such traps in the form of Na^+ cations by injecting hydrated electrons into aqueous NaCl electrolyte solutions with different salt concentrations. Hydrated electrons have a blue-shifted absorption spectrum in the presence of dissolved salts, with the magnitude of the spectral blue-shift depending on both the salt concentration and the cation identity.²⁷ We (and others²⁸) have performed MQC simulations that showed that the blue-shifted spectrum in electrolyte solutions results from the formation of (cation, e^-) contact pairs, where the electron is bound to a nearby cation (or possibly more than one cation²⁹) by several $k_{\text{B}}T$ of free energy.³⁰ Thus, for a hydrated electron to equilibrate in an electrolyte solution, the

Received: July 18, 2022

Accepted: September 1, 2022

electron must eventually end up with at least one and possibly several cation(s) located in its first solvation shell, constituting a trap relative to localization in pure water.

In this work, we present a combination of ultrafast spectroscopy experiments and MQC simulations that show that injected hydrated electrons follow trap-seeking behavior. We use the shift of the electron's absorption spectrum as a marker for whether or not there are cation(s), and thus traps, in the vicinity of the electrons as they localize. Solvation in ionic solutions is generally slower than in neat solvents because the ions need to translationally diffuse to accommodate new charge distributions.^{31–33} We find, however, that hydrated electrons injected in the presence of salts localize in essentially the same amount of time that they do in neat water, immediately achieving their blue-shifted equilibrium spectrum. This is because e_{aq}^- 's prefer to localize in pre-existing traps near sodium cations, so that electrons prefer to localize directly in traps rather than localizing quickly and then seeking the cationic traps diffusively on longer time scales.

The basic simulation and experimental data set supporting the trap-seeking behavior of injected hydrated electrons is shown in Figure 1. In both the experiments and simulations,

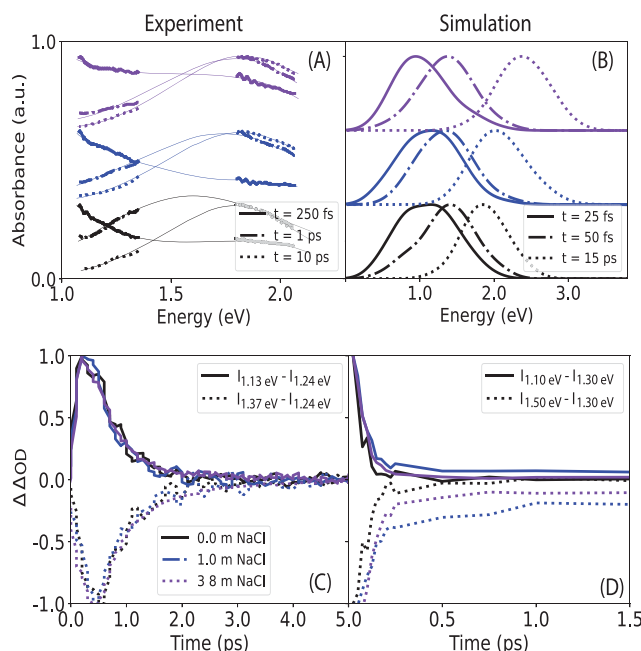


Figure 1. Spectral dynamics of hydrated electrons injected into aqueous electrolyte solutions. The top panels show the temporal evolution of the hydrated electron's absorption spectrum at short (solid curves), medium (dot-dashed curves), and longer (dotted curves) times. The bottom panels illustrate the relaxation dynamics based on the time evolution of spectral differences, as discussed in the main text. The left panels show the experimental results, collected using 4.66 eV-excited $[\text{Fe}(\text{CN})_6]^{4-}$ as the electron source; the right panels show the results from simulation. The black, blue, and purple curves correspond to 0, 1.0, and 3.8 M NaCl solutions, respectively. The thin solid curves in (A) are fits to the experimental data that are meant to guide the eye through the spectral region around 1.6 eV where we cannot collect data due to scatter from the laser fundamental; details of how these fits were produced can be found in the Supporting Information. The energy scale for the simulations is different from that for the experiments because the simulated equilibrium absorption spectrum is blue-shifted relative to experiment.³

electrons are injected into aqueous solutions with different NaCl concentrations, and the kinetics via which the electron develops its equilibrium spectrum are monitored as a function of time. In the experiments, we inject electrons by one-photon exciting the charge-transfer-to-solvent (CTTS) transition of $[\text{Fe}(\text{CN})_6]^{4-}$ at 4.66 eV (266 nm). We chose this electron source because photoexcitation ejects electrons up to 15 Å away, a similar distance to those generated via multiphoton ionization of water.³⁴ We also created electrons by multiphoton ionization of water without a specific electron source, but these attempts were complicated by the fact that multiphoton excitation can also cause electron detachment from the chloride ions in the electrolyte, which are present in high concentration. Thus, one-photon CTTS excitation provided the cleanest, most reproducible source of electron injection. In Figures S1 and S2 of the Supporting Information, we show that electrons created via CTTS excitation of $[\text{Fe}(\text{CN})_6]^{4-}$, CTTS excitation of I^- , and multiphoton excitation of water have identical localization kinetics, so that our conclusions regarding the trap-seeking behavior of the hydrated electron are robust with respect to the electron generation mechanism.

Figure 1A shows experimental transient absorption spectra of newly created hydrated electrons at delay times of 0.25 ps (solid curves, right after injection), 1 ps (dot-dashed curves, roughly halfway through the localization process), and 10 ps (dotted curves, well after the solvation process is complete) in 0 M (molality) (black curves), 1.0 M (blue curves), and 3.8 M (purple curves) NaCl solutions. Initially, when electrons are injected into solution, their absorption spectrum is broad with a peak that extends well into the near-IR, the signature of the so-called "wet" (prelocalized) electron.^{13,19} Then as the electrons become solvated, their absorption spectrum blue-shifts from the near-IR to the visible. By 10 ps, the absorption spectrum of the injected electrons matches the well-reported equilibrium spectrum of the hydrated electron. When the process takes place with 1.0 or 3.8 M of added NaCl, the equilibrium absorption spectrum of the injected electrons is identical to that in pure water other than the modest spectral blue-shift caused by the presence of the Na cation traps.²⁷

The amplified laser system in our experiments has its fundamental wavelength near 1.55 eV (800 nm), so we unfortunately cannot measure transient spectra in this region, resulting in the "missing" data in Figure 1A. Thus, to more easily visualize the spectral evolution following electron injection into the different electrolyte solutions, we examined a series of time-dependent spectral differences, $\Delta\Delta\text{OD}(t)$, which are shown in Figure 1C. To calculate the spectral differences, we first normalized the measured transient absorption dynamics of the injected electrons, $\Delta\text{OD}(t)$, at 1.13, 1.24, and 1.37 eV at a delay time of 10 ps, well after the solvation process is complete. The spectral differences were then calculated by subtracting the normalized $\Delta\text{OD}(t)$ at 1.24 eV from that at either 1.13 or 1.37 eV. We note that dynamical processes that uniformly affect the entire spectrum of the hydrated electrons, such as geminate recombination, do not appear in the spectral difference transients: the spectral differences only report on kinetic processes that change the shape of the hydrated electron's spectrum, such as the localization and solvation following injection.

Figure 1C shows that, at early times, $\Delta\Delta\text{OD}$ for 1.13 eV is positive and $\Delta\Delta\text{OD}$ for 1.37 eV is negative, indicating that the initially injected electron's absorption maximum lies to the red

of its equilibrium position, as expected for the “wet” electron. As the absorption spectrum of the injected electron blue-shifts toward equilibrium, the $\Delta\Delta\text{ODs}$ for both 1.13 and 1.37 eV decay, reaching zero after only a few picoseconds, indicating that the solvation/localization process is complete and the hydrated electron’s spectrum is at equilibrium and thus no longer changes with time. Even more importantly, however, is the fact that Figure 1C shows that, within experimental error, the relaxation dynamics of electrons injected into neat water are identical to those in 1.0 and 3.8 NaCl m solutions, despite the fact that the electrolyte solutions are 10% and 50% more viscous than neat water, respectively.³⁵

If electrons were trap-digging, they would localize in any convenient kinetically accessible spots, so that water molecules and Na^+ and Cl^- ions would have to translationally diffuse to accommodate the newly localized electron. As such hypothetical trap-digging electrons finished solvating, their absorption band would undergo an accompanying slow spectral evolution to reach the blue-shifted equilibrium position in the electrolyte solution. As we document with the simulations below, this would lead to a long-time nonzero tail or offset in the spectral differences, which we do not observe. In addition, if ion diffusion were involved, we would expect the dynamics of trap-digging electrons to be viscosity-dependent, which we also do not observe.

Instead, if injected electrons were trap-seeking, they would prefer to localize in places where there is an easy structural path to equilibration. In this case, the injected electrons would localize directly at the sites of the traps created by the sodium cations. This would cause the transient absorption spectrum to quickly reach its blue-shifted equilibrium position in the presence of salt, with no viscosity-dependent dynamics on longer time scales. Indeed, the facts that the data in Figure 1C show no difference in localization dynamics for electrons injected into 0, 1.0, and 3.8 m NaCl solutions and that the spectral differences show no long-time offsets are consistent with the conclusion that the injected electrons are trap-seeking.

To better understand why injected hydrated electrons are trap-seeking, we also performed a detailed set of non-equilibrium MQC simulations examining the injection of excess electrons into NaCl solutions with the same concentrations that we studied experimentally. The MQC methods we use are identical to those used in our previous equilibrium work on hydrated electrons in these electrolyte solutions,^{29,30} and details are given below and in the Supporting Information. We chose MQC methods because the simulation sizes and time scales needed at high salt concentrations are far too large to be accessible by ab initio techniques.

We start by examining the calculated time-dependent spectroscopy of simulated hydrated electrons injected into aqueous NaCl solutions in Figure 1B. For electrons injected into neat water, the calculated transient absorption spectra strongly resemble the experimental data in Figure 1A, but with dynamics on a faster time scale and spectra that are blue-shifted. Nearly every MQC simulation of electron injection into pure water predicts relaxation dynamics that are faster than experiment,^{3,17,36} and this is also true for our simulations here. The blue dot-dashed and purple dotted curves in Figure 1B show that the simulated localization of the electron in 1.0 and 3.8 m NaCl solutions takes the same amount of time as in neat water, in agreement with the experimental results in Figure 1A. To more directly compare to the experiments, we

show simulated spectral difference dynamics in Figure 1D, which are also in good agreement with the experiments shown in Figure 1C, other than a small slow tail/offset in the simulated data that will be discussed further below. We note that we use bluer wavelengths for the simulated spectra than the experimental spectra for this comparison because the simulated equilibrium absorption spectrum is blue-shifted,³ so that the chosen wavelengths are in a comparable position relative to the spectral maximum. The fact that the simulations indeed capture the essence of the experiments means that we can use insights from the simulations to understand the trap-seeking behavior of hydrated electron localization in electrolyte solutions.

We investigated the simulated injected electron’s trap-seeking behavior by counting the number of Na^+ ions that lie within 4.0 Å of the electron’s center of mass as a function of time, as shown in Figure 2; in other words, we examine the

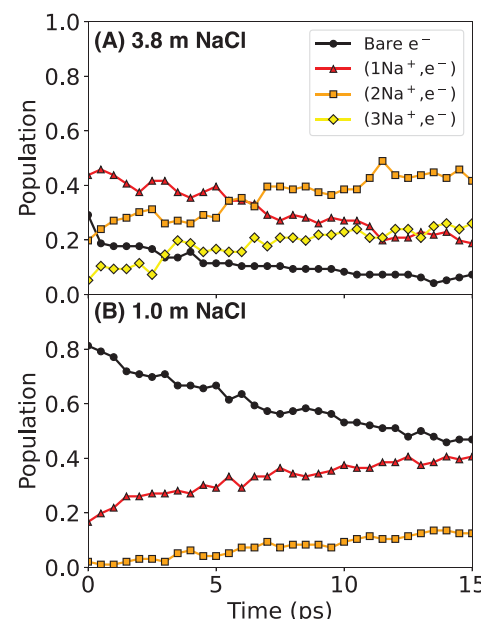


Figure 2. Simulated dynamics of cation/electron contact pair formation following electron injection into aqueous 3.8 m NaCl (panel A) and 1.0 m NaCl (panel B) solutions. Hydrated electrons that localize in a region where there are no Na^+ cations are denoted with black circles, while red triangles, orange squares, and yellow diamonds indicate $(n\text{Na}^+, e^-)$ contact pairs with $n = 1, 2, 3$, respectively.

number of cations that are close enough to participate in a contact pair with the injected electron and thus serve as traps. Distributions of the number of cations (and anions) that reside close to the electron immediately following its injection are shown in Figure S5 of the Supporting Information. As we have documented in previous work, e_{aq}^- ’s are likely to interact with multiple cations at higher salt concentrations, forming complexes that contain up to three Na^+ ions and possibly one or two Cl^- ions along with the hydrated electron.^{29,37} This is because high-concentration aqueous NaCl solutions have agglomerated Na^+/Cl^- contact ion pairs, so that pre-existing traps with multiple cations are available as localization sites for an injected electron, as shown in Figure S4.

In analyzing Figure 2, we need to note that, to reach equilibrium, the simulated electron should have ~ 2 nearby cations at 1.0 m NaCl concentration and ~ 2.5 nearby cations

with 3.8 m of salt.²⁹ Although the way in which the number of nearby cations changes with time depends on the salt concentration, it is the relative abundance of nearby Na^+ 's at the moment of injection that determines the rate at which equilibrium is achieved. The data in Figure 2 show that simulated electrons in the 3.8 m NaCl solution approach equilibrium more rapidly than those in the 1.0 m solution because the simulated electrons can more immediately form the $(2\text{Na}^+, e^-)$ and $(3\text{Na}^+, e^-)$ contact-pair species that predominate at equilibrium. Even in the high-concentration salt solutions, however, a certain fraction of the simulated injected electrons ($\sim 80\%$ at 1.0 m, $\sim 30\%$ at 3.8 m) does not start in a contact pair with any sodium cations, and another significant fraction ($\sim 20\%$ at 1.0 m, $\sim 40\%$ at 3.8 m) starts nearby only a single Na^+ . For these simulated electrons that initially localize near zero or one Na^+ , diffusive motions are needed to allow the eventual formation of the equilibrium species with multiple cations paired with the e_{aq}^- . It is these diffusive motions that are responsible for the long-time offsets in the simulated spectral differences observed in Figure 1D.

The experimental data shown in panels A and C of Figure 1 do not show a small long-time spectral shift like that predicted by the simulations. One possibility for the discrepancy is that there actually is a long-time offset for the experimental difference spectra, but it is not observable within our signal-to-noise. More likely, however, is the possibility that the simulations overexaggerate the importance of contact pairs with multiple cations, so that the experimental equilibrium involves mostly contact pairs with only a single Na^+ that are kinetically easier to achieve. Indeed, in previous work, we found that subtle changes in the classical cation/water interactions used in the simulations could dramatically affect the simulated stability of (Na^+, e^-) contact pairs³⁰ and, thus, also the distribution of multiple cation/electron pairs at equilibrium. In addition, the simulations start with the electron in the lowest adiabatic state of the water conduction band, which may not be delocalized enough to be able to “sample” the presence of proximal sodium cations: in other words, the initial adiabatic state we simulate does not extend for the ~ 15 Å ejection distance experimentally associated with the CTTS excitation of $[\text{Fe}(\text{CN})_6]^{4-}$ ³⁴ causing the simulations to underestimate the number of electrons that find Na^+ traps at early times.

At this stage, it is not possible for us to determine which of these scenarios—missing a small longer-time spectral shift in the experiments, overemphasizing the role of multiple cations in contact pairs in the simulations, or underestimating the spatial extent of the injected electron’s wave function—is correct. However, what we will argue next is that no matter which of these explanations is correct, both the experiments and simulations still support the conclusion that the injected electron is primarily trap-seeking rather than trap-digging.

Although the simulations predict that the dynamics of forming multiple-cation contact pairs can be kinetically limited by ion diffusion, particularly at intermediate salt concentrations, we can gain insight into the rate at which simulated injected electrons equilibrate by investigating how quickly $(n\text{Na}^+, e^-)$ contact pairs ($n = 1, 2$ or 3) relax once they are formed. We characterize the way these different contact pairs relax via nonequilibrium solvent response functions, $S_n(t)$, according to

$$S_n(t) = \frac{\langle U_n(t) \rangle_{\text{ne}} - \langle U_n(\infty) \rangle_{\text{ne}}}{\langle U_n(0) \rangle_{\text{ne}} - \langle U_n(\infty) \rangle_{\text{ne}}} \quad (1)$$

where $U_n(t)$ is the simulated eigenenergy of the relaxing electron with n Na^+ neighbors at time t , and $U_n(\infty)$ is the equilibrated eigenenergy of each $(n\text{Na}^+, e^-)$ species.²⁹ The subscript “ne” indicates that this quantity is a nonequilibrium ensemble average over the 96 injection trajectories we ran in each NaCl solution. In our calculation of $S_n(t)$, if the number of cations associated with the electron, n , changes from what it was initially, we remove those trajectories from the non-equilibrium ensemble. Thus, $S_n(t)$ measures the relaxation of injected hydrated electrons localizing directly near n Na^+ ions without any subsequent ionic diffusion.

Figure 3 shows these solvent response functions for each contact-pair species in both the 1.0 and 3.8 m aqueous NaCl

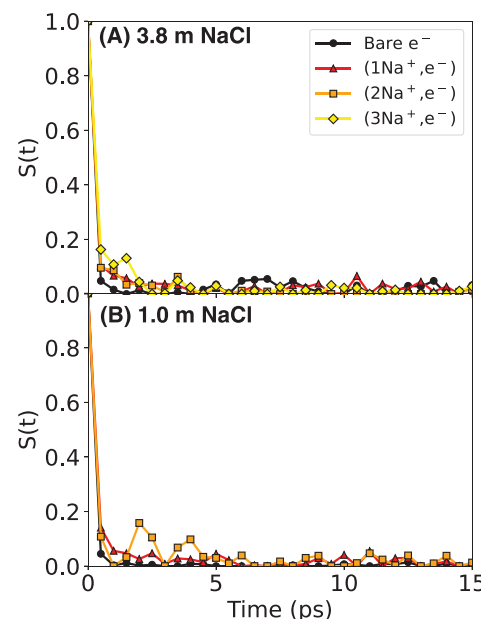


Figure 3. Simulated nonequilibrium solvent response functions (eq 1) for injected hydrated electrons that immediately form $(n\text{Na}^+, e^-)$ contact pairs with $n = 0, 1, 2, 3$ (black circles, red triangles, orange squares, and yellow diamonds, respectively) in both 3.8 m NaCl (panel A) and 1.0 m NaCl (panel B) solutions. There are too few $(3\text{Na}^+, e^-)$ in the 1.0 m NaCl solution to provide decent statistics. The data show clearly that the time for the electron to relax is essentially independent of whether or not it localizes next to one more Na^+ cation, a hallmark of trap-seeking behavior.

solutions. Independent of the electrolyte concentration, all three $(n\text{Na}^+, e^-)$ contact-pair species show relaxation dynamics that are very similar to those of the bare hydrated electron. There may be a small relaxational slowdown associated with the electrons that form two- (orange squares) and three- (yellow diamonds) cation contact pairs; this slowdown is because the cations in these complexes tend to favor linear and trigonal planar arrangements around the hydrated electron at equilibrium²⁹ that require some time to form from the initial solution geometry prior to injection. But no matter how many cations are involved and no matter what the salt concentration, at least 90% of the solvent relaxation associated with injected electrons that form ion pairs takes place in the same amount of time as for an electron in pure water. In other words, the simulations show that if the electron “lands” near one (or

more) Na^+ cations, it localizes and produces its blue-shifted spectrum with the exact same kinetics as electrons localizing in pure water. This is exactly what is observed experimentally, suggesting that no matter how many cations are involved in the final equilibrium species, injected hydrated electrons are trap-seeking.

In summary, the long-time tail observed for the simulated spectral differences in Figure 1D is due to the fraction of simulated trap-digging electrons that did not localize near a Na^+ and thus needed to diffuse to find and pair with a Na^+ to reach equilibrium. However, in the experiments (Figure 1C and Figures S1 and S2 in the Supporting Information), no matter what the electron source, the injected electrons always appear immediately with their fully blue-shifted spectrum; the lack of any long-time offset in the experimental spectral differences indicates that hydrated electrons prefer to localize directly in a contact pair “trap” with one or more sodium cations. Of course, we cannot prove with certainty that this trap-seeking behavior takes place in the absence of Na^+ , since without the cations there is no extra spectral relaxation to probe the electron’s location relative to a trap. The fact that the solvation rate is identical with and without Na^+ in both the experiments and simulations (and that we would expect solvent motions in the ionic solution to be significantly slower than those in pure water due to the ion-induced viscosity increase), however, strongly indicates that the localization and solvation mechanism is likely the same in the two cases, that is, electrons are trap-seeking both with and without electrolytes in liquid water.

EXPERIMENTAL METHODS

The data shown above used electrons injected into the room-temperature electrolyte solutions by exciting the charge-transfer-to-solvent transition of 10 mM $[\text{Fe}(\text{CN})_6]^{4-}$ by one-photon absorption at 4.66 eV. As described in more detail in the Supporting Information, we also used two-photon excitation of 10 mM I^- at 2.48 eV as well as two-photon ionization of water itself (possibly accompanied by two-photon ionization of Cl^- in the electrolyte) at 4.66 eV. Although there are differences in the long-time electron recombination dynamics with the three different ways of generating the electrons, the initial localization dynamics were indistinguishable within the experimental error. The pump/probe spectroscopy setup was the same as in our previous work studying the temperature dependence of e_{aq}^- relaxation.³⁸ Briefly, the laser system (Coherent Legend) produced ~ 3 mJ pulses of ~ 50 fs duration at 1.55 eV with a 1 kHz repetition rate. Nonlinear optical crystals were used to create the pump light, and a white-light continuum generated in either a sapphire or CaF_2 plate was used as the broadband probe. Detection was performed using a Helios (Ultrafast Systems) transient absorption spectrometer, and the sample was flowed through a 2 mm cell at a rate sufficient to ensure a fresh volume on every laser shot.

COMPUTATIONAL METHODS

Our simulations consist of a periodic box with Ewald electrostatics and many hundreds of SPC-flex water molecules³⁹ with the desired number of classical Na^+ and Cl^- ions in the microcanonical (N, V, E) ensemble with a temperature of ~ 300 K and the volume chosen to reproduce the experimental density at 1 atm. Ninety-six 15 ps nonequilibrium

trajectories at each NaCl concentration were initiated by injecting an initially delocalized single quantum-mechanical electron, represented in a basis of $24 \times 24 \times 24$ grid points into the solution in the lowest adiabatic eigenstate. We used the pseudopotential developed by Turi and Borgis³ (TB) to describe the water-electron interactions and in-house developed^{29,30,40} Phillips-Kleinman (PK) pseudopotentials⁴¹ to describe the ion-electron interactions. The velocity Verlet algorithm⁴² was used with a 0.5 fs time step to propagate the dynamics, with the quantum mechanical forces evaluated via the Hellman-Feynman theorem. Additional details are summarized in Table 1.

Table 1. Parameters for the Nonequilibrium Simulation Trajectories Studied in This Work

molality	H_2O	NaCl	box length (Å)	grid spacing (Å)
0.0	499	0	24.65	0.747
1.0	481	9	24.49	0.742
3.8	439	30	24.34	0.738

ASSOCIATED CONTENT

SI Supporting Information

The Supporting Information is available free of charge at <https://pubs.acs.org/doi/10.1021/acs.jpcllett.2c02243>.

Experimental Details and Fits to the Experimental Spectrum, Computational Details, Electron–Ion Interactions, Simulated Spectroscopy, Classical Ion–Water Interactions (PDF)

AUTHOR INFORMATION

Corresponding Author

Benjamin J. Schwartz – Department of Chemistry and Biochemistry, University of California, Los Angeles, Los Angeles, California 90095-1569, United States; orcid.org/0000-0003-3257-9152; Email: schwartz@chem.ucla.edu

Authors

Wilberth A. Narvaez – Department of Chemistry and Biochemistry, University of California, Los Angeles, Los Angeles, California 90095-1569, United States

Eric C. Wu – Department of Chemistry and Biochemistry, University of California, Los Angeles, Los Angeles, California 90095-1569, United States

Sanghyun J. Park – Department of Chemistry and Biochemistry, University of California, Los Angeles, Los Angeles, California 90095-1569, United States

Mariah Gomez – Department of Chemistry and Biochemistry, University of California, Los Angeles, Los Angeles, California 90095-1569, United States

Complete contact information is available at: <https://pubs.acs.org/10.1021/acs.jpcllett.2c02243>

Notes

The authors declare no competing financial interest.

ACKNOWLEDGMENTS

This work was supported by the National Science Foundation under Grant No. CHE-1856050. Computational resources were provided by the UCLA Institute for Digital Research and

Education and by XSEDE under computational Project No. CHE-170065.

■ REFERENCES

- (1) Hart, E. J.; Boag, J. W. Absorption Spectrum of the Hydrated Electron in Water and in Aqueous Solutions. *J. Am. Chem. Soc.* **1962**, *84*, 4090–4095.
- (2) Schnitker, J.; Rossky, P. J. An Electron–Water Pseudopotential for Condensed Phase Simulation. *J. Chem. Phys.* **1987**, *86*, 3462–3470.
- (3) Turi, L.; Borgis, D. Analytical Investigations of an Electron–Water Molecule Pseudopotential. II. Development of a New Pair Potential and Molecular Dynamics Simulations. *J. Chem. Phys.* **2002**, *117*, 6186–6195.
- (4) Jacobson, L. D.; Herbert, J. M. A One-Electron Model for the Aqueous Electron that Includes Many-Body Electron-Water Polarization: Bulk Equilibrium Structure, Vertical Electron Binding Energy, and Optical Absorption Spectrum. *J. Chem. Phys.* **2010**, *133*, 154506.
- (5) Larsen, R. E.; Glover, W. J.; Schwartz, B. J. Does the Hydrated Electron Occupy a Cavity? *Science* (80-) **2010**, *329*, 65–69.
- (6) Glover, W. J.; Schwartz, B. J. Short-Range Electron Correlation Stabilizes Noncavity Solvation of the Hydrated Electron. *J. Chem. Theory Comput.* **2016**, *12*, 5117–5131.
- (7) Uhlig, F.; Marsalek, O.; Jungwirth, P. Unraveling the Complex Nature of the Hydrated Electron. *J. Phys. Chem. Lett.* **2012**, *3*, 3071–3075.
- (8) Ambrosio, F.; Miceli, G.; Pasquarello, A. Electronic Levels of Excess Electrons in Liquid Water. *J. Phys. Chem. Lett.* **2017**, *8*, 2055–2059.
- (9) Dasgupta, S.; Rana, B.; Herbert, J. M. Ab Initio Investigation of the Resonance Raman Spectrum of the Hydrated Electron. *J. Phys. Chem. B* **2019**, *123*, 8074–8085.
- (10) Park, S. J.; Schwartz, B. J. Evaluating Simple Ab Initio Models of the Hydrated Electron: The Role of Dynamical Fluctuations. *J. Phys. Chem. B* **2020**, *124*, 9592–9603.
- (11) Shen, Z.; Peng, S.; Glover, W. J. Flexible Boundary Layer Using Exchange for Embedding Theories. II. QM/MM Dynamics of the Hydrated Electron. *J. Chem. Phys.* **2021**, *155*, 224113.
- (12) Migus, A.; Gauduel, Y.; Martin, J. L.; Antonetti, A. Excess Electrons in Liquid Water: First Evidence of a Prehydrated State with Femtosecond Lifetime. *Phys. Rev. Lett.* **1987**, *58*, 1559–1562.
- (13) Long, F. H.; Lu, H.; Eisenenthal, K. B. Femtosecond Studies of the Presolvated Electron: An Excited State of the Solvated Electron? *Phys. Rev. Lett.* **1990**, *64*, 1469–1472.
- (14) Kambhampati, P.; Son, D. H.; Kee, T. W.; Barbara, P. F. Solvation Dynamics of the Hydrated Electron Depends on Its Initial Degree of Electron Delocalization. *J. Phys. Chem. A* **2002**, *106*, 2374–2378.
- (15) Savolainen, J.; Uhlig, F.; Ahmed, S.; Hamm, P.; Jungwirth, P. Direct Observation of the Collapse of the Delocalized Excess Electron in Water. *Nat. Chem.* **2014**, *6*, 697–701.
- (16) Kee, T. W.; Son, D. H.; Kambhampati, P.; Barbara, P. F. A Unified Electron Transfer Model for the Different Precursors and Excited States of the Hydrated Electron. *J. Phys. Chem. A* **2001**, *105*, 8434–8439.
- (17) Webster, F. J.; Schnitker, J.; Friedrichs, M. S.; Friesner, R. A.; Rossky, P. J. Solvation Dynamics of the Hydrated electron: A Nonadiabatic Quantum Simulation. *Phys. Rev. Lett.* **1991**, *66*, 3172–3175.
- (18) Schwartz, B. J.; Rossky, P. J. Pump–Probe Spectroscopy of the Hydrated Electron: A Quantum Molecular Dynamics Simulation. *J. Chem. Phys.* **1994**, *101*, 6917–6926.
- (19) Pizzochero, M.; Ambrosio, F.; Pasquarello, A. Picture of the Wet Electron: A Localized Transient State in Liquid Water. *Chem. Sci.* **2019**, *10*, 7442–7448.
- (20) Schnitker, J.; Rossky, P. J.; Kenney-Wallace, G. A. Electron Localization in Liquid Water: A Computer Simulation Study of Microscopic Trapping Sites. *J. Chem. Phys.* **1986**, *85*, 2986–2998.
- (21) Motakabbir, K. A.; Rossky, P. J. On the Nature of Pre-Existing States for an Excess Electron in Water. *Chem. Phys.* **1989**, *129*, 253–262.
- (22) Bartczak, W. M.; Pernal, K. Potential Traps for an Excess Electron in Liquid Water: the Trap Lifetime Distributions. *Res. Chem. Intermed.* **2001**, *27*, 891–900.
- (23) Nordlund, D.; Ogasawara, H.; Bluhm, H.; Takahashi, O.; Odelius, M.; Nagasono, M.; Pettersson, L. G. M.; Nilsson, A. Probing the Electron Delocalization in Liquid Water and Ice at Attosecond Time Scales. *Phys. Rev. Lett.* **2007**, *99*, 217406.
- (24) Glover, W. J.; Larsen, R. E.; Schwartz, B. J. Simulating the Formation of Sodium:Electron Tight-Contact Pairs: Watching the Solvation of Atoms in Liquids One Molecule at a Time. *J. Phys. Chem. A* **2011**, *115*, 5887–5894.
- (25) Bragg, A. E.; Kanu, G. U.; Schwartz, B. J. Nanometer-Scale Phase Separation and Preferential Solvation in THF–Water Mixtures: Ultrafast Electron Hydration and Recombination Dynamics Following CTTS Excitation of I-. *J. Phys. Chem. Lett.* **2011**, *2*, 2797–2804.
- (26) Bahry, T.; Denisov, S. A.; Moisy, P.; Ma, J.; Mostafavi, M. Real-Time Observation of Solvation Dynamics of Electron in Actinide Extraction Binary Solutions of Water and n-Tributyl Phosphate. *J. Phys. Chem. B* **2021**, *125*, 3843–3849.
- (27) Bonin, J.; Lampre, I.; Mostafavi, M. Absorption Spectrum of the Hydrated Electron Paired with Nonreactive Metal Cations. *Radiat. Phys. Chem.* **2005**, *74*, 288–296.
- (28) Coudert, F.-X.; Archirel, P.; Boutin, A. Molecular Dynamics Simulations of Electron-Alkali Cation Pairs in Bulk Water. *J. Phys. Chem. B* **2006**, *110*, 607–615.
- (29) Narvaez, W. A.; Park, S. J.; Schwartz, B. J. Hydrated Electrons in High-Concentration Electrolytes Interact with Multiple Cations: A Simulation Study. *J. Phys. Chem. B* **2022**, *126*, 3748–3757.
- (30) Park, S. J.; Narvaez, W. A.; Schwartz, B. J. How Water–Ion Interactions Control the Formation of Hydrated Electron:Sodium Cation Contact Pairs. *J. Phys. Chem. B* **2021**, *125*, 13027–13040.
- (31) Smith, D. E.; Dang, L. X. Computer Simulations of NaCl Association in Polarizable Water. *J. Chem. Phys.* **1994**, *100*, 3757–3766.
- (32) Collins, K. D.; Neilson, G. W.; Enderby, J. E. Ions in Water: Characterizing the Forces that Control Chemical Processes and Biological Structure. *Biophys. Chem.* **2007**, *128*, 95–104.
- (33) Fumino, K.; Stange, P.; Fossog, V.; Hempelmann, R.; Ludwig, R. Equilibrium of Contact and Solvent-Separated Ion Pairs in Mixtures of Protic Ionic Liquids and Molecular Solvents Controlled by Polarity. *Angew. Chemie Int. Ed.* **2013**, *52*, 12439–12442.
- (34) Kloepfer, J. A.; Vilchez, V. H.; Lenchenkov, V. A.; Bradforth, S. E. *ACS Symp. Ser.* **2002**, *820*, 108–121.
- (35) Kestin, J.; Khalifa, H. E.; Correia, R. J. Tables of the dynamic and kinematic viscosity of aqueous NaCl solutions in the temperature range 20–150 °C and the pressure range 0.1–35 MPa. *J. Phys. Chem. Ref. Data* **1981**, *10*, 71–88.
- (36) Keszei, E.; Nagy, S.; Murphrey, T. H.; Rossky, P. J. Kinetic Analysis of Computer Experiments on Electron Hydration Dynamics. *J. Chem. Phys.* **1993**, *99*, 2004–2011.
- (37) Bartczak, W. M.; Kroh, J.; Zapalowski, M.; Pernal, K. Computer Simulation of Water and Concentrated Ionic Solutions. Potential Fluctuations and Electron Localization. *Philos. Trans. R. Soc. London. Ser. A Math. Phys. Eng. Sci.* **2001**, *359*, 1593–1609.
- (38) Farr, E. P.; Zho, C.-C.; Challa, J. R.; Schwartz, B. J. Temperature dependence of the hydrated electron's excited-state relaxation. II. Elucidating the relaxation mechanism through ultrafast transient absorption and stimulated emission spectroscopy. *J. Chem. Phys.* **2017**, *147*, 139903.
- (39) Toukan, K.; Rahman, A. Molecular-Dynamics Study of Atomic Motions in Water. *Phys. Rev. B* **1985**, *31*, 2643–2648.
- (40) Glover, W. J.; Larsen, R. E.; Schwartz, B. J. The Roles of Electronic Exchange and Correlation in Charge-Transfer-to-Solvent Dynamics: Many-Electron Nonadiabatic Mixed Quantum/Classical Simulations of Photoexcited Sodium Anions in the Condensed Phase. *J. Chem. Phys.* **2008**, *129*, 164505.

(41) Smallwood, C. J.; Larsen, R. E.; Glover, W. J.; Schwartz, B. J. A Computationally Efficient Exact Pseudopotential Method. I. Analytic Reformulation of the Phillips-Kleinman Theory. *J. Chem. Phys.* **2006**, *125*, 074102.

(42) Verlet, L. Computer "Experiments" on Classical Fluids. I. Thermodynamical Properties of Lennard-Jones Molecules. *Phys. Rev.* **1967**, *159*, 98–103.